

Mechanical Behaviors and Deformation Properties of Retaining Wall Formed by Grouting Mould-Bag Pile

Shengcai Li^{1,*}, Jun Tang^{1,2} and Lin Guo³

Abstract: The simplified mechanical model and finite element model are established on the basis of the measured results and analysis of the grouting pile deformation monitoring, surface horizontal displacement and vertical displacement monitoring, deep horizontal displacement (inclinometer) monitoring, soil pressure monitoring and seepage pressure monitoring in the lower reaches of Wuan River regulation project in Shishi, Fujian Province. The mechanical behavior and deformation performance of mould-bag pile retaining wall formed after controlled cement grouting in the silty stratum of the test section are analyzed and compared. The results show that the use of controlled cement grouting mould-bag pile technology is to strengthen the soft stratum for sealing water and reinforcement, so that it can rock into a retaining wall, which can both retain soil and seal water with excellent effect. The control of cement grouting technology not only makes the soft soil rock in the range of retaining wall of mould-bag pile, but also makes a wide range of soil around the mould-bag pile squeeze and embed to compaction; and its cohesion and internal friction angle increased, so as to achieve the purpose of reducing soil pressure and improving mechanical and deformation properties of retaining wall.

Keywords: Controlled cement grouting technology, grouting mould-bag pile, retaining wall, mechanical behaviors, deformation properties.

1 Introduction

The regulation project in the lower reaches of Wuan River in Shishi of Fujian Province involves soft silty stratum, buildings or structures nearby, and underground box-culverts in the governance range, which brings difficulties to construction. The original design adopts double-row cast-in-place pile, which is easy to cause collapse with high cost. Afterwards, it was decided to adopt the composite structure of controlled cement grouting mould-bag pile and silt hardening body to form retaining wall for river regulation. However, this technology has not been applied in similar projects. Whether

¹ School of Civil Engineering, Huaqiao University, Xiamen, 361021, China.

² Cross-strait Tsinghua Research Institute, Xiamen, 361006, China.

³ Fujian Engineering Research Center for Construction and Management of Green Buildings, Minnan University of Science and Technology, Quanzhou, 362700, China.

* Corresponding Author: Shengcai Li. Email: lsc50605@hqu.edu.cn.

high-pressure grouting will cause displacement or even damage to the box-culvert; whether the retaining wall can withstand the earth pressure after excavation, and how about its sealing and seepage prevention effect are not clear, all need to be verified in the test section.

The forming principle of the “controlled cement grouting mould-bag pile” is that the high-strength mould-bag is bound in the grouting pipe and loaded into the hole, and the grout is injected into the mould-bag through the controlled cement grouting. With the enlargement of the mould-bag pile, the cylindrical pile equivalent to the diameter of the mould-bag is formed. The soft strata outside the mould-bag piles (such as quicksand bed, soft soil stratum, soft rock stratum, karst, fault fracture zone, and more) are compressed. The liquid and gas phases in the soft strata are discharged from the surface through the ground cracks and pre-embedded drainage facilities, and the soft strata within the affected area are consolidated to a certain extent.

The “controlled cement grouting mould-bag pile” technology is used to seal and reinforce the soft stratum and make it rock to form retaining wall. This kind of retaining wall can not only retain soil but also seal water. It has been verified by the lower reaches of Wu’an River regulation project in Shishi, Fujian Province with excellent effect. Rocking technology not only makes the soft soil in the retaining wall of the mould-bag pile rock, but also makes a wide range of soil around the mould-bag pile squeeze and embed to compaction, and the cohesion and internal friction angle increase to reduce the earth pressure of retaining wall.

The bearing capacity of bored prestressed concrete hollow pile with large-diameter is studied in document [Feng and Xie (2005)]. The bearing capacity of various post-grouting cast-in-place piles is studied in Liu et al. [Liu, Wang and Liu (2016); Fang, Zhang and Liu (2012)], and the mechanical and deformation properties of various retaining walls are studied in Wang et al. [Wang, Yang and Yan (2017); Liu, Hu and Pan (2013); Zhou, Xie and Jiang et al. (2015)]. Taking the newly-built inter-city railway extension project from Zhengzhou to Jiaozuo as an example, the cement grouting method is adopted to deal with the areas with insufficient bearing capacity in the project. Due to site constraints, combined with the characteristics of silty soil foundation in this section, small drilling machine was used to drill holes and insert steel pipes. After grouting, the unplugged steel pipe is combined with soil and cement. The mechanism of grouting reinforcement is analyzed. The bearing capacity of composite foundation after grouting is calculated by using the bearing capacity calculation method of steel pipe pile. Comparing indoor and field static load tests, the bearing capacity of foundation calculated by this method was close to the test results [Wang, Wang, Wen et al. (2015)]. In view of the development of joints and fissures in a copper mine and the extremely fractured surrounding rock of the orebody, a large number of reinforcement and support are needed, and the ultra-fine cement grouting technology was firstly selected [Wu, Yu, Han et al. (2014)]. Based on the orthogonal design, laboratory tests and theoretical studies were carried out to optimize the mix proportion for different water cement ratio (W/C) and cement slurry/water glass volume ratio (C/S). The optimum water cement ratio (W/C) and cement slurry/water glass volume ratio (C/S) meeting the requirements of grouting strength were proposed, and field grouting tests were carried out based on

the recommended grouting solution mix ratio. The parameters such as grouting pressure and diffusion radius have been determined, and the grouting process system has been built. The fault zones caused jamming of the TBM cutterhead and shield. Ground improvement and grouting techniques were implemented widely to release TBM. Applied techniques were fully successful and the TBM restarted excavation after eight months stoppage [Bayati and Hamidi (2017)]. Q-logging system was developed based on the cores drilled at the grouting panels to investigate the influence of the cement grouting on the rock mass properties at the Bakhtiary dam site. In this way, rock masses in different boreholes at the grouting panels were classified using the Q-system. Then, using the experimental equations, rock mass deformation modulus (E_{rm}) was calculated for each borehole. In order to evaluate this method, value of the rock mass deformation modulus was also obtained by the dilatometer test results. The outcomes display that the Q-logging system can be used as a practical and undemanding method in evaluation of rock mass quality by the grouting treatment [Zolfaghari, Bidar, Javan et al. (2015)]. The mechanical behaviors of drainage pipeline under traffic load before and after polymer grouting and cement grouting trenchless repairing are investigated through three-dimensional (3D) finite element method (FEM). Four different working conditions, including normal pipeline, disengaging pipeline, polymer-repaired pipeline, and cement-repaired pipeline were considered. The effects of load type, load location, buried depth on the mechanics of pipe are discussed in detail [Fang, Li, Wang et al. (2018)]. In order to achieve a great grouting effect for the case with flowing water, carbon fiber was added to the cement grout and a new grout for flowing water environment was provided, and a series of grouting test in the fracture with flowing water was conducted. Effects of plastic viscosity, flowing water velocity, grouting pressure and roughness coefficient of joint on the propagation of carbon fiber composite cement grout was analyzed [Yang, Li, Song et al. (2016)]. Grouting-based treatment technology was presented for tunnel settlement in the soft deposits of Shanghai, China. The aim of the grouting treatment was to control the development of the tunnel settlement. The mechanism of settlement control through grouting was presented. A dual-fluid system of cement and sodium silicate was adopted in the proposed grouting-based treatment technology. A new front-end device is designed specially to avoid blocking the grouting holes. The grouting parameters are determined based on field tests and engineering practices [Zhang, Huang, Wang et al. (2018)]. Grouting process of quick setting slurry in a single horizontal fissure was studied. The step-wise calculation method is proposed to describe the grouting process, considering the uneven distribution of slurry viscosity in grouted zone. The circular grouted zone was divided into infinitesimal annular elements, according to the moment when the slurry particle was injected into the fissure from the injection hole. Case studies of two conditions (constant grouting flow and constant grouting pressure) were investigated to capture the distribution of slurry viscosity and pressure in grouted zone. Fissure grouting test was performed to verify that the developed step-wise calculation method was suitable for the analysis of the distribution of pressure in grouted zone [Zhang, Zhang, Liu et al. (2017)]. Based on the engineering background of the sand-layer collapse disaster in Qingdao Metro Line 2, detailed analysis of the process and mechanism of sand-layer collapse in tunnels was done. Grouting method was used to improve collapse-preventing treatment in the sand layer.

For treating the water-bearing sand layer above the tunnel, an advancement of grouting reinforcement system was proposed. The results showed that the main causes of sand-layer collapse are the intrinsic characteristics of the sand layer itself. The cohesive soil content of the sand layer is low and the cementation ability of the sand layer is weak. The advancing grouting method applied in this project is an effective method to strengthen the sand layer; the grouting parameters obtained in this study can be used as a guidance for similar engineering projects [Wu, Wang, Zhang et al. (2018)]. The southern slope of Chengmenshan copper minewas divided into six sections (I-0, I-1, I-2, II-0, II-1 and II-2) for slope stability analysis using limit equilibrium and numerical method. Stability results showed that the values of factor of safety (FOS) of sections I-0, I-1 and I-2 were very low and slope failure was likely to happen. Therefore, reinforcement subjected to seismic, water and weak layer according to sections were carried out to increase the safety of the three sections, and two methods were used; grouting with hydration of cement and water to increase the cohesion (c) and pre-stressed anchor [Mohammed, Wan and Wei (2015)]. Bohlooli et al. [Bohlooli, Morgan, Grø et al. (2018)] describes a systematic laboratory study to characterize uniaxial compressive strength (UCS) and filtration stability of grouts made up of three types of cement commonly used for tunnel grouting in the Nordic countries. Since in-situ tunnel conditions are different from those of the laboratory in terms of temperature, we made various cement grouts at different temperatures and tested in the laboratory. The water cement ratios of 0.6, 0.8, 1.0 and 1.2 were used for all three cements and grouts were made and cured at two temperatures: 8°C and 20°C. Strength of a total of 96 cylindrical specimens of 4- and 7-days age and permeability of four specimens of 7 days age were measured. Filtration tests were done for 36 cement grouts. Reference [Zhang, Fang and Lou (2014)] presents a case study of Xiang'an subsea tunnel in Xiamen, the first subsea tunnel in China. During its construction, different grades of weathered geomaterials were encountered, which was the challenging issue for this project. To deal with these unfavorable geological conditions, grouting was adopted as an important measure for ground treatment. The grouting mechanism is first illustrated by introducing a typical grouting process. Then the site-specific grouting techniques employed in the Xiang'an subsea tunnel are elaborated. There are four main characteristics for a grout mixture including bleeding, setting time, strength, and viscosity [Mohammad, Ali and Ali (2017)]. In this paper, we try to build some efficient grouting mixtures with different water to cement ratios considering these characteristics. The ingredients of grout mixtures built in this study are cement, water, bentonite, and some chemical additives such as sodium silicate, sodium carbonate, and triethanolamine (TEA). The grout mixtures are prepared for both of the sealing and strengthening purposes for a structural project. Effect of each abovementioned ingredient is profoundly investigated. In Li et al. [Li, Liu, Zhang et al. (2016)], the current situation of control and prevention of water and mud inrush is summarized and recent advances in relevant theories, grout/equipment, and critical techniques are introduced. The time-variant equations of grout viscosity at different volumetric ratios were obtained based on the constitutive relation of typical fast curing grouts. A large-scale dynamic grouting model testing system (4000 mm×2000 mm×5 mm) was developed, and the diffusions of cement and fast curing grouts in dynamic water grouting were investigated.

Chen [Chen (2018)] presents a combined construction technology that has been developed for use in underground spaces; it includes a deformation buffer layer, a special grouting technique, jump excavation by compartment, back-pressure portal frame technology, a reinforcement technique, and the technology of a steel portioning drum or plate. These technologies have been successfully used in practical engineering. The combined construction technology presented in this paper provides a new method of solving key technical problems in underground spaces in effectively used cross-subway tunnels. Fan et al. [Fan, Wang and Qian (2018)] reviews and discusses the general classifications of grouting techniques and the suitability of their applications. The mechanical properties of soil-cement mixture and the influence of sodium silicate added are discussed. Design considerations for deep soil mixed wall (DSMW) for excavation support and vault arch for tunneling stabilization are presented. Parameters for the numerical analysis of soil-cement mixture are evaluated and recommended. Merkin et al. [Merkin, Konyukhov, Simutin et al. (2016)] presents technique of regulated constructing elevation of buildings after their settlement because of tunneling under them. Control of buildings' elevation is based on preliminary calculation of grouting zones positions, injection sequence and injection volumes. Special software complex performs control functions over compensation grouting process, and coordinating pumps work according to permanent horizontal and vertical monitoring of fundaments and correcting technological parameters of compensation grouting. However, the analysis of the force and deformation of the retaining wall formed by the "controlled cement grouting bag pile" technology has not yet been reported [Xiao, Xing and Li (2000); Liang and Jiang (2011)]. Therefore, this paper intends to analyze the force and deformation properties of the retaining wall formed by the "controlled cement grouting bag pile" technology for reference in the applications of engineering.

2 Analysis of real-time monitoring results in test section

2.1 Monitoring items and main contents

The main contents of the monitoring project are:

- (1) Enclosure structure monitoring: deformation monitoring of grouting hole pile.
- (2) Surrounding soil monitoring: 1) Surface horizontal displacement and vertical displacement monitoring. 2) Deep horizontal displacement (inclinometer) Monitoring. 3) Soil pressure monitoring. 4) Seepage pressure monitoring.

2.2 Layout of measuring points and observation method

- (1) Monitoring section: The length of the test section is 10 m, and 3 monitoring sections are arranged. The pile numbers are 3#, 9# and 15# respectively.
- (2) Layout of measuring points: the monitoring section is equipped with grouting hole pile concrete strain gauge, the surface horizontal and vertical displacement mark points, inclinometer tube, earth pressure cell, osmometer and other instruments. According to the principle of less but better, the layout of measuring points is not only representative, but also can reflect the deformation of grouting body, the change of foundation settlement and horizontal displacement, the increase and dissipation of pore water

pressure, and the change of soil pressure during the construction. The layout of measuring points is shown in Fig. 1 and Fig. 2.

During the test stage of the foundation pit excavation, seven observation points L1-L7 were evenly arranged on the top girder of the mould-bag pile with a length of 10.5 m to monitor the horizontal and vertical displacement of the pile top, shown in Fig. 3.

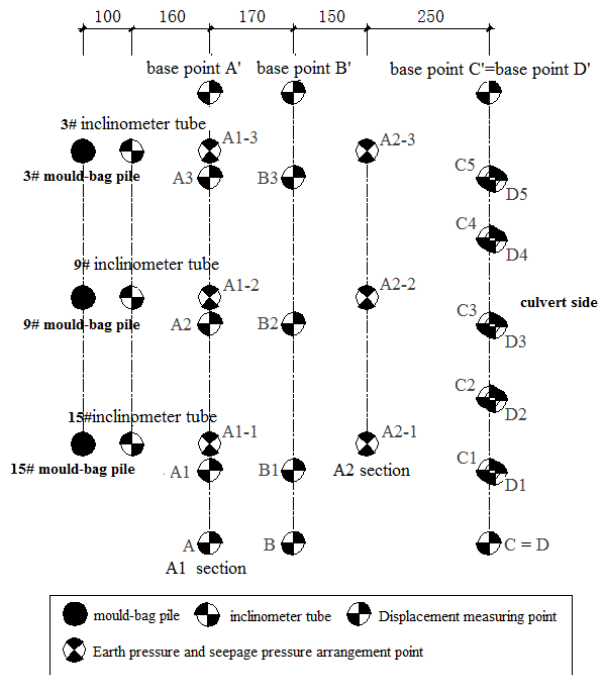


Figure 1: The floor plan of measuring point

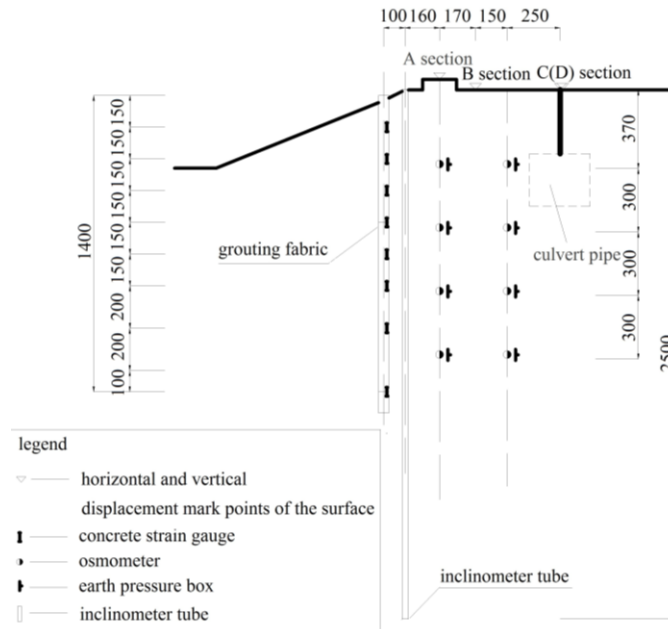


Figure 2: The profile layout of measuring point

(3) Monitoring methods and instruments:

1) The surface horizontal displacement

The surface horizontal displacement is measured by the collimation method. When controlling the line of sight, the check point must be located outside the deformation area, and the deviation value near the displacement measuring points of the respective stations must be observed. The optical alignment of the instrument is less than 0.5 mm. Each monitoring should be observed at least two times, each time including the forward and backward mirror observation, and “double-reference” observation was used; that is, two times of the targets and micrometer reading respectively. The mean value is taken as the measured value of the measurement. The difference between the two readings of positive or inverted mirrors is ± 4 mm, and the difference between the two measurements is ± 3 mm.

2) The surface vertical displacement

The surface vertical displacement is carried out by observing the vertical displacement of the points. The DSZ2 automatic leveling precision level is used to observe the surface vertical displacement. The standard deviation of the instrument is ± 1.0 mm, and the readings can reach 0.01 m. The leveling base point is located in the place where the position of the point is stable, not be destroyed by the construction and the line of sight is not obstructed during the whole period of observation.

3) Observation of deep horizontal displacement (inclinometer)

The JTM-U6000FA intelligent vertical inclinometer of Changzhou Golden Civil Engineering Instrument Co.; Ltd. of Jiangsu Province is used for deep horizontal displacement observation, as shown in Fig. 4. The inclinometer consists of a probe, a cable and a receiving instrument. The sensor of the inclinometer probe adopts a servo accelerometer with high sensitivity, high accuracy and good long-term stability. The inclinometer tube is embedded in the observation position. The inclinometer is a flexible PVC pipe embedded in the soil. The whole pipe deforms with the deformation of the foundation and is in harmony with the horizontal deformation of the foundation. The inclinometer is used to measure the inclinometer of each point in the pipeline, and the displacement of the silt and the silty clay layer in the foundation is mastered. The observation results mainly include the distribution of horizontal displacement along the depth, the magnitude and location of the maximum horizontal displacement of soil, the change rate of horizontal displacement and more. The resolution of the inclinometer is 0.01 mm/500 mm and the accuracy is ± 2 mm/20 m.

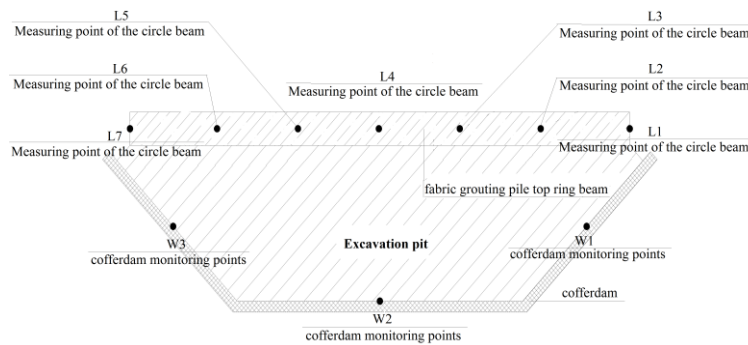


Figure 3: The layout of measuring point in the foundation pit excavation



Figure 4: Intelligent movable vertical inclinometer

4) Observation of strain gauge, earth pressure cell and osmometer

The strain gauge, earth pressure cell and osmometer are all vibrating wire sensors of Jiangsu Changzhou Gold Civil Engineering Instrument Co.; Ltd. The models are JTM-V5000, JTM-V2000 and JTM-V3000, respectively, as shown in Fig. 5. It has the advantages of short time lag, sensitive reaction, good long-term stability, high waterproof performance and little temperature effect. The working principle is that the bellows (or pressure modes) are used as elastic elements. When the bellows (or pressure modes) produce small linear deformation, the natural vibration frequency of the

vibrating string pressure sensor changes. The pore water pressure value can be calculated by measuring the natural vibration frequency of the vibrating string. Its accuracy is less than or equal to 2.0% F.S.

2.3 Field monitoring results and analysis

2.3.1 Horizontal and vertical displacement of girder surface at the top of pile



Figure 5: Concrete strain meter, earth pressure cell and osmometer

After pit excavation of the foundation on November 14, 2016, the horizontal displacement and elevation change process lines of each section were drawn after continuous observation and statistics is shown in Fig. 6 and Fig. 7. Positive value in the displacement map indicates to move to the center of the foundation pit, and the positive value in the elevation map indicates downward settlement.

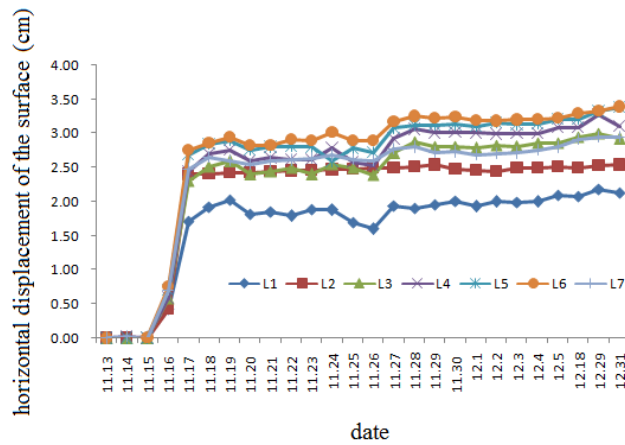


Figure 6: The hydrograph of horizontal displacement of girder surface at the top of pile

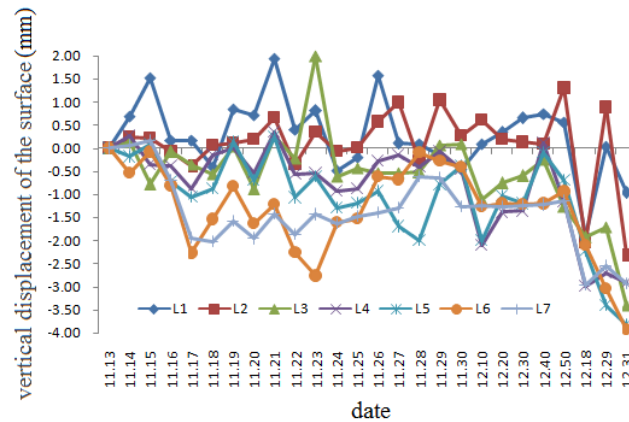


Figure 7: The hydrograph of the vertical displacement of girder surface at the top of pile

In particular, it must be noted that during the construction of cable-stayed piles from November 16 to 17, due to the continuous maintenance of high-pressure grouting, there is no sectional grouting, which results in a displacement variation of more than 20 mm at the girder surface, as detailed in Fig. 6. This is caused by improper construction method, and strict sectional grouting method and grouting pressure control measures should be adopted to prevent out-of-control deformation. In addition, it can be seen from the above figures that for most of the rest of November 18, the horizontal displacement of the surface and the vertical displacement of the surface are very limited (no more than 4 mm, within the allowable range of error) with the excavation of the foundation pit. It shows that the composite structure of bag pile and mud hardened body formed by high pressure-controlled cement grouting has optimal envelope effect and can ensure engineering safety. At the same time, it is also indicated that the ground pressure released after excavation is very small, resulting in very little deformation of the pile.

2.3.2 The surface horizontal displacement

After continuous observation for a period of time, the horizontal displacement process line of section A is drawn after statistics. As shown in Fig. 8, the positive value indicates the deviation towards the box culvert, while the negative value is opposite.

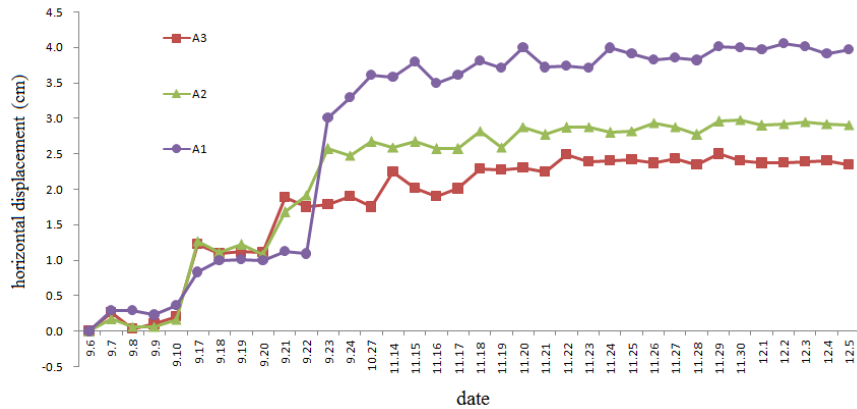


Figure 8: Hydrograph of the horizontal displacement in section A

From the above Fig. 8, it can be seen that the surface horizontal displacement in each section changes relatively large during September 18-21, the main reason is that it was in the period of pile grouting construction. In addition, because section A is located nearest to the pile, the surface horizontal displacement is relatively large, and the maximum value reaches 40 mm. A1, A2 and A3 are closest to grouting holes, and are most affected by grouting.

After the excavation of foundation pit on November 14, especially after the grouting construction of cable-stayed piles on November 18, it can be seen from Fig. 8 that the horizontal displacement of each measuring point is not large (less than 3 mm) and the development trend is stable, which shows that the retaining effect of mould-bag piles is optimal, and that the ground pressure released after the excavation of foundation pit is very small.

2.3.3 Deep horizontal displacement (inclinometer)

Deep horizontal displacement is observed by inclinometer tube. There are 3 holes to put the inclinometer tube, which are arranged at 1m from 3#, 9# and 15# piles respectively. After continuous observation and statistics, the deep horizontal displacement (inclination measurement) of each hole position is plotted. The positive value indicates the deviation towards the box culvert, while the negative value is opposite as shown in Figs. 9-12.

It can be seen from the diagram that the variation of horizontal displacement along the depth of each hole is similar. The displacement of each hole is almost unchanged when it is in the depth of the hole bottom. With the decrease of the depth, the displacement increases gradually. When the depth is about 2 m, the displacement of each hole reaches its peak, and the maximum horizontal displacement of the 9# hole is 338 m. The deep horizontal displacement of each hole is mainly affected by grouting construction. After grouting, the trend is more stable, and the change is generally small. In addition, due to the influence of blank holes (borehole diameter 20 cm) formed by burring the borehole, the variation of deep horizontal displacement is also large at the initial stage of observation.

After the excavation of the foundation pit on November 14, especially after the grouting construction of the cable-stayed piles on November 18, the deep horizontal displacement of each hole changes little with stable development trend. It shows that the influence of foundation pit excavation on the surrounding area is limited; the envelope effect of mould-bag pile is optimal and the ground pressure released after foundation pit excavation is very small. Safety is guaranteed.

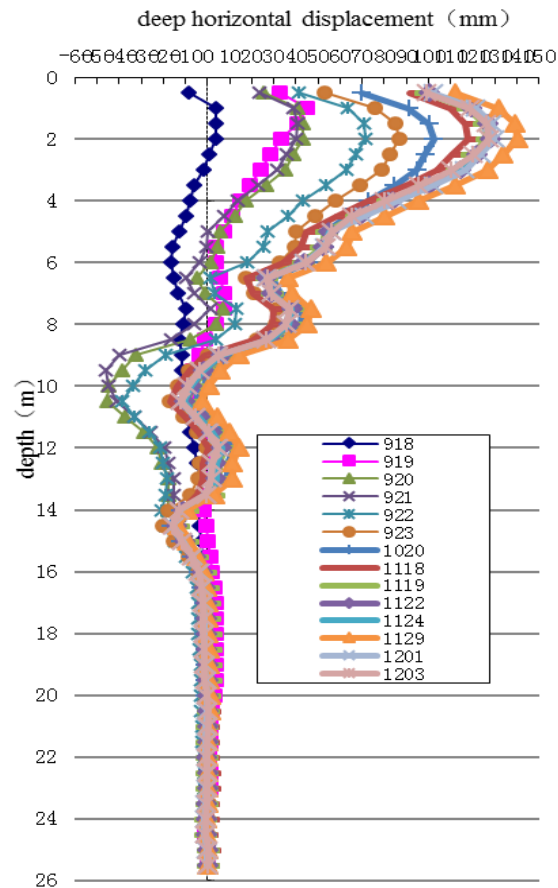


Figure 9: Deep horizontal displacement in 3#

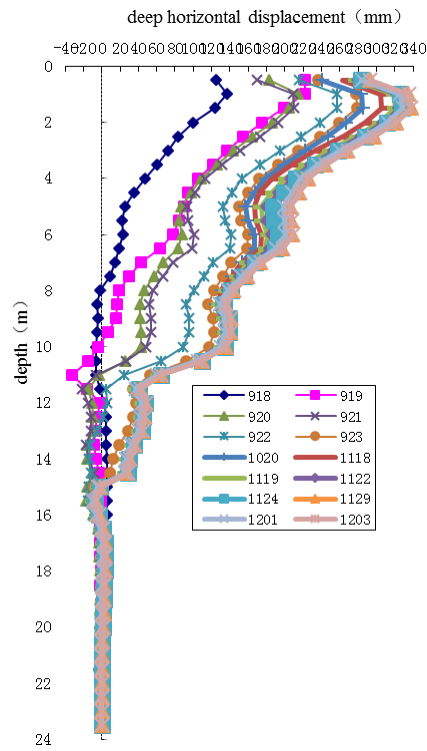


Figure 10: Deep horizontal displacement in 9#

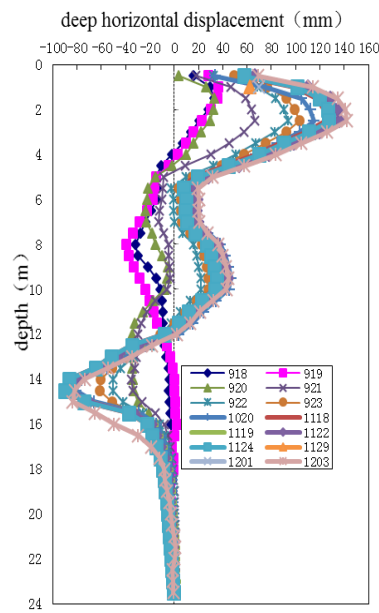


Figure 11: Deep horizontal displacement in 15#

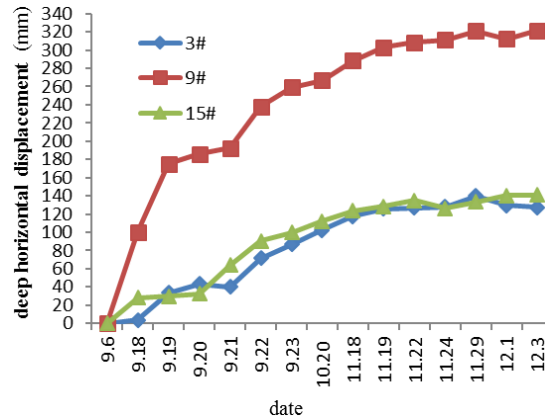


Figure 12: Hydrograph of the deep horizontal displacement for each hole with 2 m depth

2.3.4 Concrete strain

Concrete strain adopts vibrating wire strain gauge to measure. One strain gauge is arranged at the depths of 1.5 m, 3 m, 4.5 m, 6 m, 7.5 m, 9 m, 11 m and 13 m respectively at 3 #, 9 # and 15 #, and 8 strain gauges are arranged at each hole. Concrete strain process line in 9# is drawn after statistics. As shown in Fig. 13.

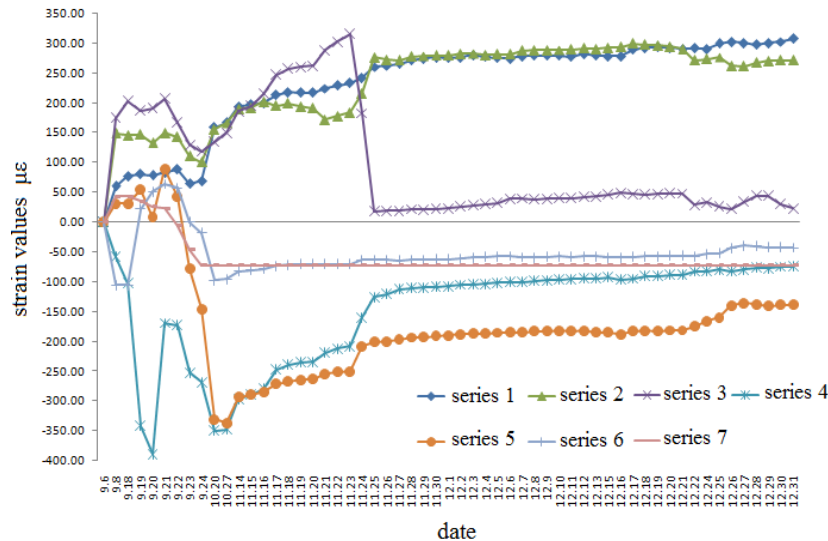


Figure 13: the hydrograph of concrete strain in 9#

It can be seen from Fig. 13 that the concrete strain is mainly affected by the grouting construction. After the grouting, especially after November 25 and the excavation of the foundation pit is stable, the trend is very gentle, and the overall change is not large, which indicates that the ground pressure release is very small after excavation.

2.3.5 Earth pressure and seepage pressure

For the monitoring of earth pressure and seepage pressure, this project arranges two monitoring sections, A1 and A2, which are 2.6 m and 5.8 m away from the grouting holes axis respectively. Each section has three holes. One earth pressure cell and one osmometer are arranged for each hole at the depths of 3.7 m, 6.7 m, 9.7 m and 12.7 m respectively, which are marked as series 1 to series 8 (odd as earth pressure cell and even as osmometer).

From the variation of earth pressure and seepage pressure (Figs. 14 and 15), it can be seen that the earth pressure and seepage pressure are related to the buried depth of the test point. The deeper the depth is, the greater the earth pressure and seepage pressure are. At the same time, it is also affected by grouting pressure, and the earth pressure and seepage pressure increase immediately during grouting. After grouting, the earth pressure and seepage pressure gradually dissipate and tend to be stable. The excavation has little effect on the earth pressure and seepage pressure, that is, after the foundation pit excavation, the earth pressure and seepage pressure basically remain unchanged with no release.

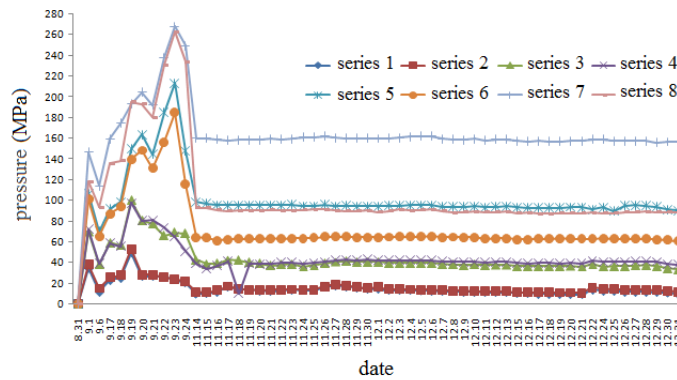


Figure 14: The curve of soil pressure and seepage pressure in A1-2

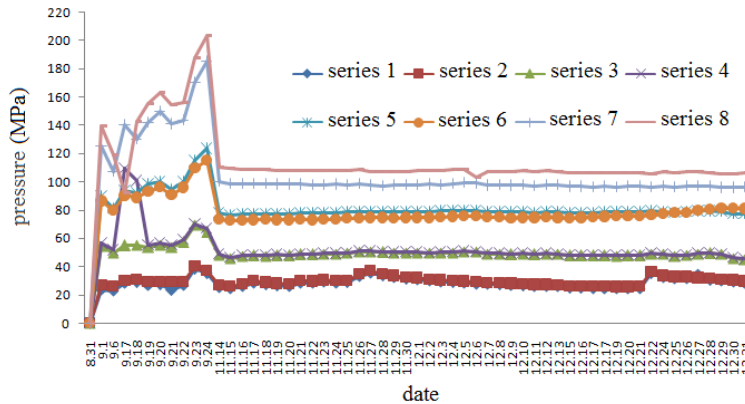


Figure 15: The curve of soil pressure and seepage pressure in A2-2

3 Internal force analysis of retaining wall

3.1 Simplified mechanical model

The reinforcement of the right bank embankment test section in the downstream regulation project of Wuan River in Shishi is shown in Fig. 16. The reinforcement and support are to use the composite structure technology of mould-bag pile and silt hardening body to reinforce the embankment as a whole and play the role of water sealing and slope protection. In order to analyze and evaluate the reinforcement effect of composite structure, the following simplified mechanical model is established for analysis: the upper cable-stayed piles are supported by movable hinge bearing, and the bottom of the mould-bag pile (15 meters) is taken as the fixed bearing and the fixed hinge bearing (two extremes) respectively. Because the buried depth is large and the surrounding soil is compacted during the bottom grouting process, there will be no horizontal movement of the pile bottom (this can be confirmed by the deep horizontal displacement test results (Figs. 9~11)), and the most dangerous situation is rotation. The soil outside the pile in the excavation depth (0~5 m) range is calculated by active earth pressure, and the earth pressure inside the pile is zero; the soil outside the pile below 5 m~10 m range is calculated by active earth pressure; the soil pressure inside the pile is calculated by passive earth pressure; the soil in the excavation depth below 10 m~15 m range is calculated by static earth pressure on both sides of the pile, and a single pile is taken for theoretical calculation. The ground pressure is calculated according to the soil mass after grouting.

3.2 Calculation of ground pressure

According to the soil test results table, the actual soil and geological prospecting report in the construction section are quite different. In order to facilitate analysis and calculation, the actual soil is simplified into clay and silty clay as shown in Tab. 1.

Table 1: Soil and physico-mechanical index

layer No.	soil name	layer thickness/m	unit weight /(kN/m^3)	cohesion / kPa	internal friction angle/($^\circ$)
1	clay	5	18.95	22.22	18.03
2	silty clay	10	16.83	7.57	19.23

The earth pressure calculated according to the actual excavation property is shown in Tab. 2.

Table 2: Calculation results of earth pressure

layer No.	soil	soil and water	soil pressure outside the pile/kPa	soil pressure inside the pile/kPa
1	clay	together	upper-21.84, take to 0; lower 28.38	upper 0; lower 0
2	silty clay	together	upper 46.63;	upper 21.35;

	(5~10 m)		lower 88.70	lower 187.80
3	silty clay	at rest	upper 133.26;	upper 56.38;
	(10~15 m)	earth	lower 189.64	lower 112.76

3.3 Internal force calculation of retaining wall

According to the maximum load test results of pull-out test, the pull-out pile with depth of 4m can bear 80 kN tensile force under the same conditions. Therefore, the restraint condition at the cable-stayed pile can be assumed as a movable hinge bearing. The pile bottom is simplified to the fixed bearing, and the mechanical model of the mould-bag pile is shown in Fig. 17.

Solving a single statically indeterminate structure, the internal force of the mould-bag pile is obtained as shown in Fig. 18. Maximum bending moment and maximum shear force are both at the bottom of the pile. Maximum bending moment value outside the pile is 134.96 kNm; maximum bending moment value inside the pile is 86.34 kNm; and maximum shear force is 142.96 kN.

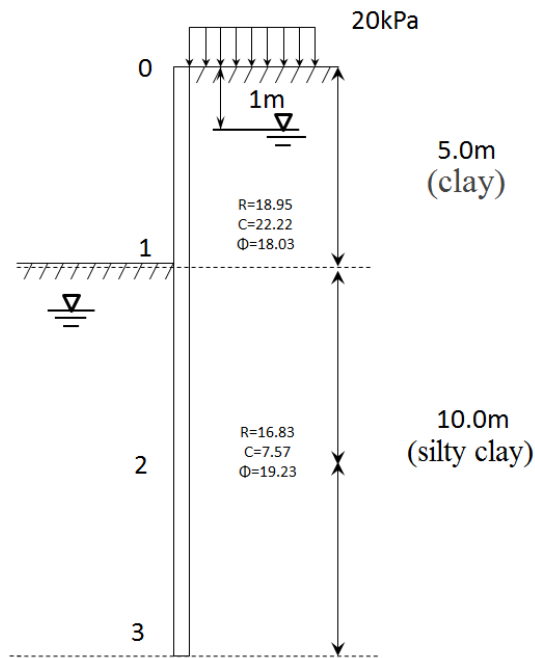


Figure 16: Interface sketch of main mould-bag pile

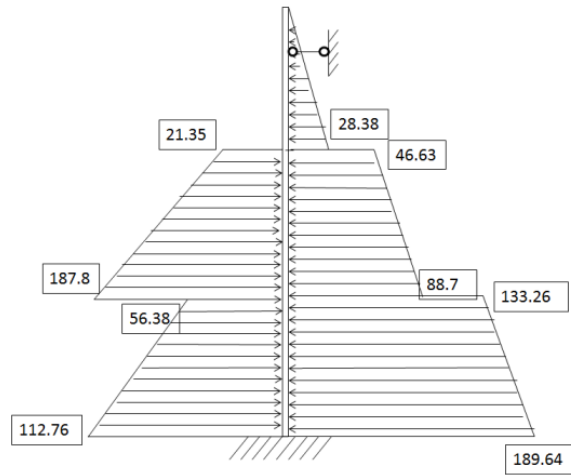


Figure 17: Simplified calculation diagram of pile bottom with fixed end

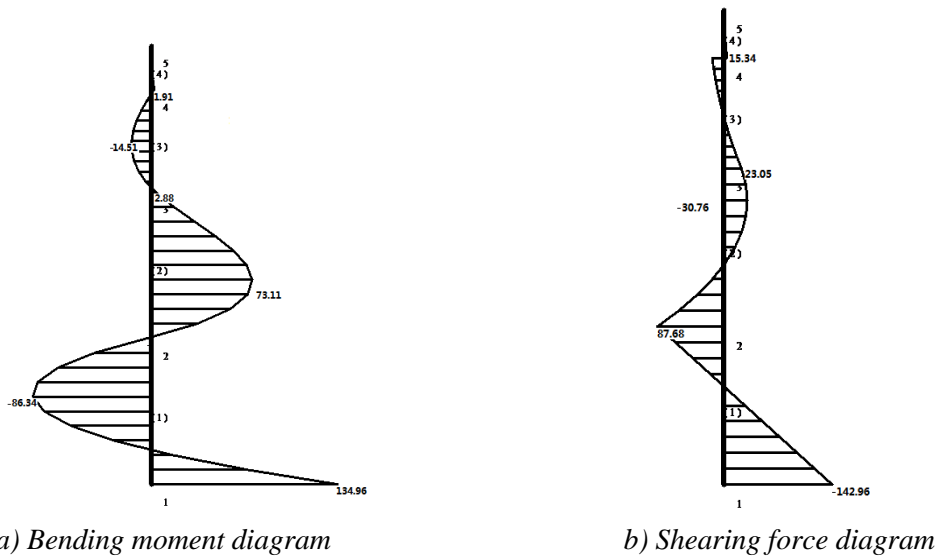


Figure 18: Internal force diagram of pile bottom with fixed end

The pile bottom is simplified to the fixed hinge bearing, and the mechanical model of the mould-bag pile is shown in Fig. 19. The internal force of the pile is calculated as shown in Fig. 20. Maximum shear force is at the bottom of the pile. Its value is 132.96 kN. Maximum bending moment value outside the pile is 9.04 kNm; maximum bending moment value inside the pile is 191.31 kNm.

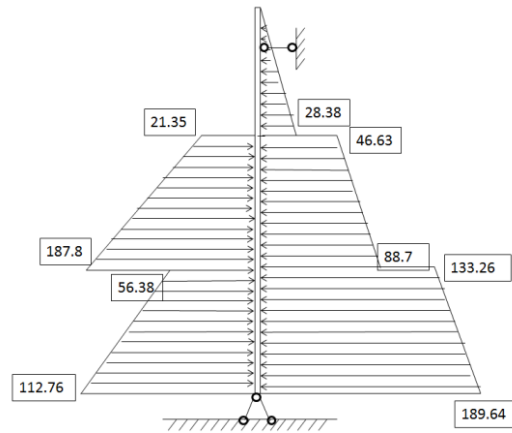


Figure 19: Simplified calculation diagram of pile bottom with fixed hinged support

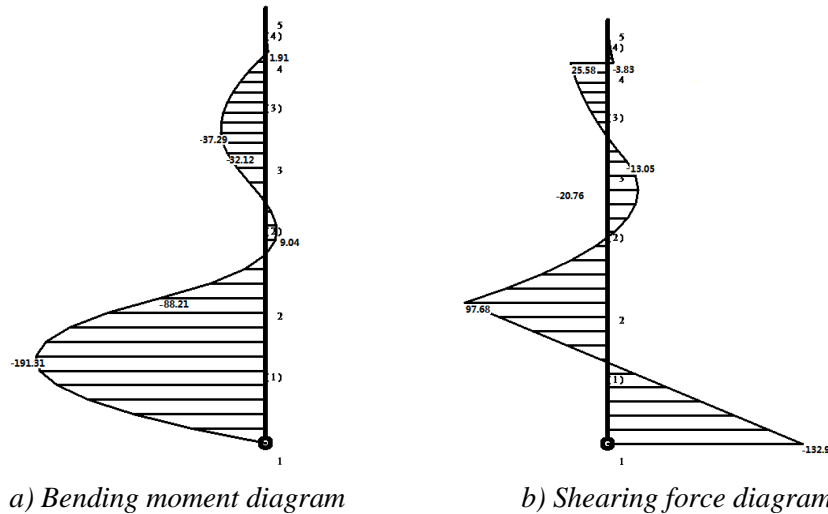


Figure 20: Internal force diagram of pile bottom with fixed hinged support

3.4 Internal forces in finite element calculation

3.4.1 Modeling and calculation process

- 1) According to the dimensional drawing confirmed by the right bank embankment test section in the downstream regulation project of Wuxi River in Shishi, ABAQUS commercial software is used to build element model; using 2D modelling, the cable-stayed pile is equivalent to beam element. Its element is shown in Fig. 21.
- 2) The material attributes of soil, pile and cable-stayed pile are assigned to the corresponding parts. Since the purpose of this model is to calculate the moment of the pile, the material attributes of the pile and cable-stayed pile are simplified to C30 concrete.
- 3) Define the analysis step. The analysis step named ‘geo’ is first defined, and

'procedure' is set as 'geostatic', whose purpose is to balance the in-situ stress.

4) Assembling. Only the earth element is assembled this time as shown in Fig. 22.

5) Set boundary conditions and loads as shown in Fig. 23. The displacement of X direction is restricted by both sides and middle of the soil, and the displacement of Y direction is restricted by the bottom of the soil. A uniform load is set on the left side and in the middle of the soil body to make it equivalent to the excavation in order to balance the ground stress when the vertical force is applied.

6) Mesh generation. The pile body is divided into 90 elements and 124 nodes. Together with the surrounding soil, there are 1950 elements and 2098 nodes as shown in Fig. 24.

7) Submit the calculation. The stress files of the soil are calculated and processed. The resulting stress file is assigned to the 'keywords' inserted in the statement. To ensure that the displacement of the soil in the Y direction is almost negligible.

8) Define the analysis step. Create an analysis step called 'con'. Procedure is set to 'static' and 'general'. The analysis step is shown in Fig. 25.

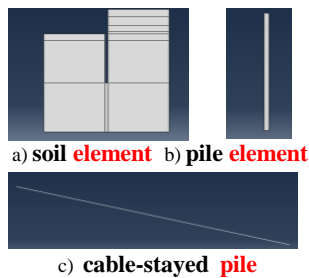


Figure 21: Element construction

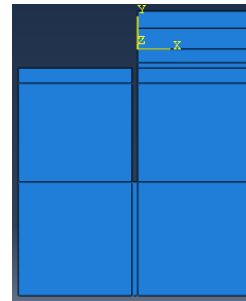


Figure 22: Soil element

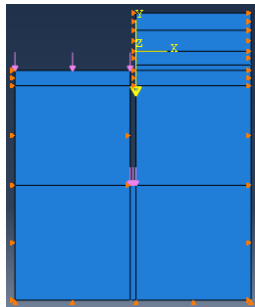


Figure 23: The load and

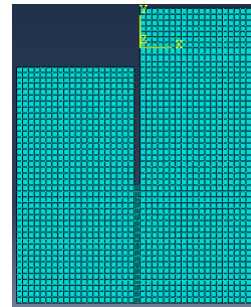


Figure 24: Mesh generation boundary conditions of soil

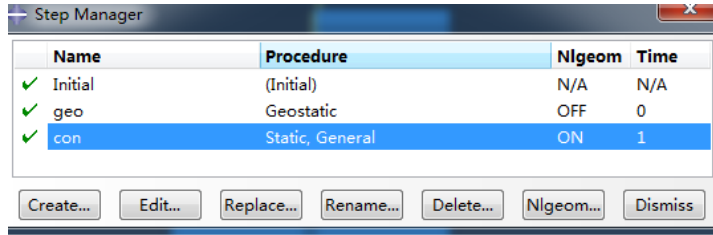


Figure 25: Analysis steps

- 9) Assembling. Assemble the cable-stayed pile and the mould-bag pile to the corresponding position, as shown in Fig. 26.
- 10) Definition of load. The corresponding load and boundary conditions are defined to the corresponding positions and analysis steps. At the same time, a uniform load named 'you' is applied to the upper right side of the soil, and the bottom of the pile is set to restrict the displacement of Y direction as shown in Figs. 27~28.
- 11) Define the interactions. The normal direction of pile and soil is set as hard contact, and the tangential direction defines a friction coefficient (the friction coefficient is determined by literature). The pile and the cable-stayed pile are set as tie constraints of point to point; the cable-stayed pile is set as the whole model embedded in the soil, and the pile bottom and the corresponding soil contact define a tie constraint in order to make the pile bottom and the corresponding soil section bound together.
- 12) The whole is divided into element meshes.
- 13) Calculation. The corresponding bending moments of piles are calculated and processed. The bending moment diagram is shown in Fig. 29.

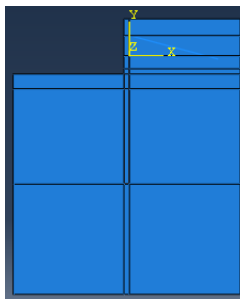


Figure 26: Assembling (model)

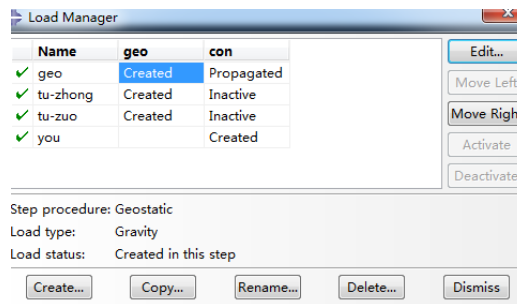
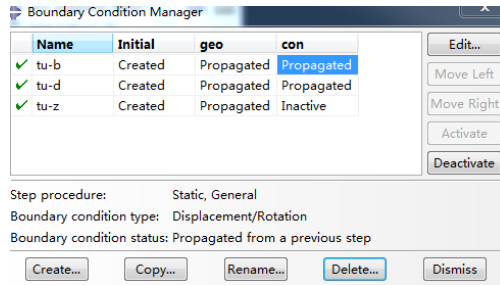
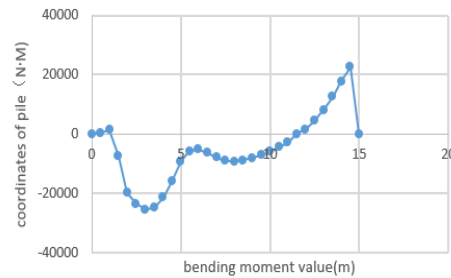


Figure 27: Load definition

**Figure 28:** Boundary condition definition**Figure 29:** Bending moment diagram of the pile

3.4.2 Analysis of finite element calculation results

It can be seen from the bending moment diagram (Fig. 29) that the maximum bending moment is only 25.5 kNm, and the flexural requirements can be satisfied according to the structural reinforcement. Because the shear force is very small, the concrete is strong enough to resist shear, thus there is no need for shear reinforcement.

4 Conclusion

(1) Since the excavation of foundation pit on November 14, 2016, especially after the completion of grouting construction of cable-stayed piles on November 17 and 18, the observed values of horizontal and vertical displacement of girder surface at the top of pile, the surface horizontal displacement, deep horizontal displacement (inclinometer), earth pressure, seepage pressure and concrete strain have not changed largely as a whole, and the development trend is gentle, which shows foundation pit excavation has limited influence on the surrounding area, and the retaining effect of mould-bag pile is optimal, which also shows that the ground pressure released after foundation pit excavation is very small. Safety is guaranteed.

(2) According to the changes of displacement, pressure and strain of each measuring point after the excavation of foundation pit, the ground pressure changes very little after the excavation of foundation pit in the allowable range of error. Therefore, after the foundation pit excavation, only very small bending moment and shear force will be produced to the mould-bag pile forming the retaining wall, which is due to the production in the process of grouting. A great deal of pressure is generated, which makes the surrounding soil compacted, thus greatly increase the cohesion and internal friction angle of the soil around the pile, and greatly reduce the ground pressure. This is also confirmed by finite element analysis. Theory and experiment are consistent.

(3) Due to the lithification and compaction of the bag-moulded pile, the ground pressure is greatly reduced, and the bending moment and shear force are greatly reduced, so the pile used as retaining wall is not necessary for reinforcement, thus greatly reduces the cost of retaining walls. It saves engineering cost.

Acknowledgement: The work is supported by the National Natural Science Foundation of China (No. 51578253); Scientific and Technological Planning Project of Xiamen

City (Nos. 3502Z20172011 and 3502Z20172014); Scientific and Technological Planning Project of Quanzhou City (No. 2018C083R); Reform study of graduate education and teaching of Huaqiao University in 2018 (No. 18YJG55).

References

Bayati, M.; Hamidi, J. K. (2017): A case study on TBM tunnelling in fault zones and lessons learned from ground improvement. *Tunnelling and Underground Space Technology*, vol. 63, pp. 162-170.

Bohlooli, B.; Morgan, E. K.; Grøv, E.; Skjølsvold, O.; Olav Hognestad, H. (2018): Strength and filtration stability of cement grouts at room and true tunnelling temperatures. *Tunnelling and Underground Space Technology*, vol. 71, pp. 193-200.

Chen, X. S. (2018): Research on Combined Construction Technology for Cross-Subway Tunnels in Underground Spaces. *Engineering*, vol. 4, pp. 103-111.

Fan, J. G.; Wang, D. Y.; Qian, D. (2018): Soil-cement mixture properties and design considerations for reinforced excavation. *Journal of Rock Mechanics and Geotechnical Engineering*, vol. 10, pp. 1-7.

Fang, H. Y.; Li, B.; Wang, F. M.; Wang, Y. K.; Cui, C. (2018): The mechanical behavior of drainage pipeline under traffic load before and after polymer grouting trenchless repairing. *Tunnelling and Underground Space Technology*, vol. 74, pp. 185-194.

Fang, K.; Zhang, Z. M.; Liu, X. W. (2012): Prediction of bearing capacity of post grouting pile in gravel layer based on settlement criterion. *Chinese Journal of Rock Mechanics and Engineering*, vol. 31, no. 6, pp. 1178-1183 (In Chinese).

Feng, Z. J.; Xie, Y. L. (2005): Simulation test of large diameter bored hollow pile of prestressing force concrete. *Journal of Chang'an University (Natural Science Edition)*, vol. 25, no. 2, pp. 50-54 (In Chinese).

Li, S. C.; Liu, R. T.; Zhang, Q. S.; Zhang, X. (2016): Protection against water or mud inrush in tunnels by grouting: a review. *Journal of Rock Mechanics and Geotechnical Engineering*, vol. 8, pp. 753-766.

Liang, R. X.; Jiang, J. L. (2011): Comparative election of anti-seepage method for open diversion channel of Zhentouba Hydropower Station I. *Water Resources and Hydropower Engineering*, vol. 42, no. 5, pp. 84-87 (In Chinese).

Liu, G.N.; Hu, R. H.; Pan, X. H. (2013): Model tests on mechanical behaviors of sheet pile wall with relieving platform. *Chinese Journal of Geotechnical Engineering*, vol. 35, no. 1, pp. 103-110 (In Chinese).

Liu, T. J.; Wang, Y.; Liu, K. (2016): Experimental test on post grouting filling pile in collapsible loess. *Building Structure*, vol. 46, no. 16, pp. 97-100 (In Chinese).

Merkin, V.; Konyukhov, D.; Simutin, A.; Medvedev, G. (2016): Stabilizing of high-altitude position of the centrifuge's foundation by compensation grouting technique during underground tunneling. *Procedia Engineering*, vol. 165, pp. 658- 662.

Mohammad, R.A.; Ali, T.; Ali, T. (2017): Optimization of cement-based grouts using chemical additives. *Journal of Rock Mechanics and Geotechnical Engineering*, vol. 9, pp. 623-637.

Mohammed, M.; Wan, L.; Wei, Z. (2015): Slope stability analysis of Southern slope of Chengmenshan copper mine, China. *International Journal of Mining Science and Technology*, vol. 25, no. 2, pp. 171-175.

Wang, J.L.; Wang, Y.S.; Wen, P. Y. (2015): Bearing capacity formula of a cement grouting in silty soil foundation. *Journal of Hydraulic Engineering*, vol. 46, no. S1, pp. 23-26 (In Chinese).

Wang, Q. L.; Yang, X. H.; Yan, C. G. (2017): Analysis of the stress and deformation characteristics of geocell flexible retaining wall for subgrade shoulders. *Journal of Railway Science and Engineering*, vol. 14, no. 5, pp. 980-987 (In Chinese).

Wu, A.X.; Yu, S.F.; Han, B.; Wang, Y. (2014): Optimization of mix-proportion and diffusing rule of super-fine cement grouting slurry. *Journal of Mining & Safety Engineering*, vol. 31, no. 2, pp. 304-309 (In Chinese).

Wu, Y. Q.; Wang, K.; Zhang, L. Z.; Peng, S. H. (2018): Sand-layer collapse treatment: an engineering example from Qingdao Metro subway tunnel. Part 1. *Journal of Cleaner Production*, vol. 197, pp. 19-24.

Xiao, T. Y.; Xing, J. P.; Li, W. L. (2000): Experimental study on material and technology for foundation chemical grouting strengthening of Three Gorges Project. *Journal of Yangtze River Scientific Research Institute*, vol. 17, no. 6, pp. 22-24, 28 (In Chinese).

Yang, P.; Li, T. B.; Song, L.; Deng, T.; Xue, S. B. (2016): Effect of different factors on propagation of carbon fiber composite cement grout in a fracture with flowing water. *Construction and Building Materials*, vol. 121, pp. 501-506.

Zhang, D. L.; Fang, Q.; Lou, H. C. (2014): Grouting techniques for the unfavorable geological conditions of Xiang'an subsea tunnel in China. *Journal of Rock Mechanics and Geotechnical Engineering*, vol. 6, pp. 438-446.

Zhang, D. M.; Huang, Z. K.; Wang, R. L.; Yan, J. Y.; Zhang, J. (2018.): Grouting-based treatment of tunnel settlement: Practice in Shanghai. *Tunnelling and Underground Space Technology*, vol. 80, pp. 181-196.

Zhang, Q. S.; Zhang, L. Z.; Liu, R. T.; Li, S. C.; Zhang, Q. Q. (2017): Grouting mechanism of quick setting slurry in rock fissure with consideration of viscosity variation with space. *Tunnelling and Underground Space Technology*, vol. 70, pp. 262-273.

Zhou, J.; Xie, X. B.; Jiang, J. (2015): Deformation characteristics and influence factors of wrap reinforced retaining wall. *Chinese Journal of Rock Mechanics and Engineering*, vol. 34, no. 1, pp. 148-154 (In Chinese).

Zolfaghari, A.; Bidar, A. S.; Maleki Javan, M. R.; Haftani, M.; Mehinrad, A. (2015): Evaluation of rock mass improvement due to cement grouting by Q-system at Bakhtiary dam site. *International Journal of Rock Mechanics and Mining Sciences*, vol. 74, pp. 38-44.